Article:
Hare, C, Ghadiri, M orcid.org/0000-0003-0479-2845 and Wu, C-Y (2021) Discrete element modelling of ribbon milling: A comparison of approaches. Powder Technology, 388. pp. 63-69. ISSN 0032-5910

https://doi.org/10.1016/j.powtec.2021.03.071

Discrete Element Modelling of ribbon milling: a comparison of approaches

C. Hare[1], M. Ghadiri[2], Chuan-Yu Wu[1]

[1]Department of Chemical and Process Engineering, University of Surrey, Guildford, GU2 7XH, UK
[2]School of Chemical and Process Engineering, University of Leeds, Leeds LS2 9JT, UK

Abstract

Roller compaction followed by milling of the generated ribbons is a typical dry granulation route. It is desirable to be able to predict the size distribution of the granules exiting the mill based on the ribbon properties and mill operational conditions. Two DEM-PBM approaches for predicting this size distribution are compared; a direct approach where the size distribution is experimentally determined, and an indirect approach where the successive change in size distribution due to each stressing event is determined mathematically by the PBM. The experimental component of the direct approach assumes shear deformation to be the dominant breakage mechanism. This approach provides a reasonable agreement to experimental data, though the influence of mill parameters is not experimentally tested. When considering breakage to be driven by impact, the indirect approach predicts the correct magnitude of fines generation, though incorrectly predicts the fine fraction to increase with impeller speed. When abrasion is assumed to be the dominant breakage mechanism, the indirect approach suggests the same trend, though with a less pronounced effect of impeller speed and a closer agreement to experimental data. Prediction accuracy is expected to improve by considering distributions of stressing conditions and material strength, the latter being explicitly captured in the experimental component of the direct method. Furthermore, the direct method accounts for the variable loading conditions of the fragments in the mill.

Key words: DEM, particle breakage, ribbon milling, pharmaceuticals

Highlights:

- Direct and indirect DEM-PBM ribbon milling size prediction approaches are described
- The two approaches are compared and contrasted
- A critique is given on the important features of ribbon milling prediction models

1. Introduction

Many powder processes require multiple components of fine dry particles to be combined to make a suitable product. Due to the poor flow behaviour of fine particles and the need to prevent segregation, it is common to form granules through agglomeration, which thereby contain the required ratio of well-mixed powder. Both dry and wet granulation techniques are widely used, with dry granulation often being preferential if it is viable for the given process. The most common dry granulation process is roller compaction followed by milling: the powder ingredients are mixed and compressed into a sheet (known as a ‘ribbon’ or a ‘flake’) in a roller compactor, then dropped directly into a mill to break into granules that are larger than the raw materials. Ribbon mills typically comprise a hemi-cylindrical screen at the base, with side walls and a set of rotating bars or pins that contact the ribbons and shear them against each other and the base. The ribbons break

down by impacting the bars/pins and each other, as well as by being sheared directly against the screen at the base.

The properties of the ribbons, such as dimensions, porosity and strength distribution, are determined by the raw materials properties and the roller compaction process. Average ribbon density increases with peak compaction pressure and nip angle (Miguélez-Morán *et al.*, 2008; Khorasani et al., 2015). Feed materials with lower hardness provide higher density and stronger ribbons, due to the increased contact area arising during the compaction process [3]. It is desirable to be able to predict and control the size distribution of the granules exiting the mill. Within the mill the number of bars/pins and their rotational speed can be controlled, as well as the mesh size of the screen and the clearance between the bars/pins and the screen. The mesh size of the screen is highly influential in affecting the size distribution; acting as a classifier to limit the upper size of the product. A larger mesh results in a coarser product, as shown by [4] for both a co-mill and a hammer mill, with the latter providing greater precision by allowing particles close to the mesh size to exit the mill. The orientation of the mesh opening to the direction of flow in the mill is also influential, with openings unaligned to the flow minimising fines generation [5]. The influence of rotational speed of the mill on product size distribution is dependent on the mill type, with increasing speed leading to finer products in a hammer mill whilst no effect is observed in a co-mill [4]. For a given mill operational condition, the extent of size reduction can be related to the fracture energy from three-point bend tests [6]. Although several correlations have been found between material and operational parameters to product size distribution in a given mill, due to the complexity of breakage behaviour in ribbon mills it is difficult to predict the size distribution based directly on the ribbon properties and the operational conditions of the mill.

The Discrete Element Method (DEM) can be useful to predict the behaviour of particle systems, including ribbons, in response to operational conditions, with various models available to directly represent breakage within the DEM, the most common of which are:

Bonded particle method – particles are represented by multiple non-overlapping spheres that are held together by a bond. The auto-adhesive model applying a JKR contact law of defined surface energy to contacting spheres has been used to mimic experimental fragmentation and chipping behaviour [7]. An alternative approach is the cemented bond model, whereby a rigid bond with defined strength is applied between bonded spheres [8]. A key distinction between the two approaches is that bonded particles rotate as a single entity around their combined centre of mass in the latter, whilst they are free to rotate independently in the former.

Particle replacement method – each particle is represented by a single element, which is then replaced by multiple elements based on a breakage function if a threshold contact condition (e.g. stress, force or velocity) is exceeded [9]. In order for volume to be conserved in the replacement process, it is necessary to allow the progeny to initially overlap significantly, with their velocities dampened until their contact is broken, as in the approach introduced by Brosh *et al.* (2011).

Finite-Discrete Element Method (FDEM) – the DEM is used to determine the contact list, calculate contact forces and apply equations of motion to determine velocities, whilst the Finite Element Method (FEM) determines stresses and applies a breakage model. In the FEM component, particles are represented by a mesh of fine elements which are connected by a cohesive bond, with full stress analysis applied and fracture propagating along element boundaries that exceed the bond strength [11]. An alternative approach is the Scaled Boundary FDEM (SBFDEM), whereby the stress field is determined by a semi-analytical method, with a straight-line breakage path passing through the average position of points that exceed their strength [12].

An alternative approach to directly representing particle breakage in DEM simulations is to couple DEM with a Population Balance Model (PBM). With this method the DEM is used solely to provide the important contact behaviour that leads to breakage, such as impact velocities or shear stresses, whilst the breakage behaviour of this material under such conditions is determined by other means (typically experimentally) to inform the PBM. An advantage of this approach is that the DEM is less computationally expensive since the simulation is not required to run for as long, however it relies upon the assumption that the contact conditions remain relatively stable throughout the entire process, regardless of the breakage experienced by the material in the mill. Since the residence time of the broken material is very small in ribbon mills, this is a promising approach to modelling their behaviour. Two such DEM-PBM approaches have recently been applied for ribbon mills: the *direct approach* of Hare *et al.* [13] and the *indirect approach* of Loreti *et al.* [14,15]. The key steps involved in each product size distribution prediction approach are illustrated in Figure 1 and outlined individually in Sections 2 and 3 for the direct and indirect approach, respectively. In this paper we critically review the two approaches and provide recommendations for such size prediction models.

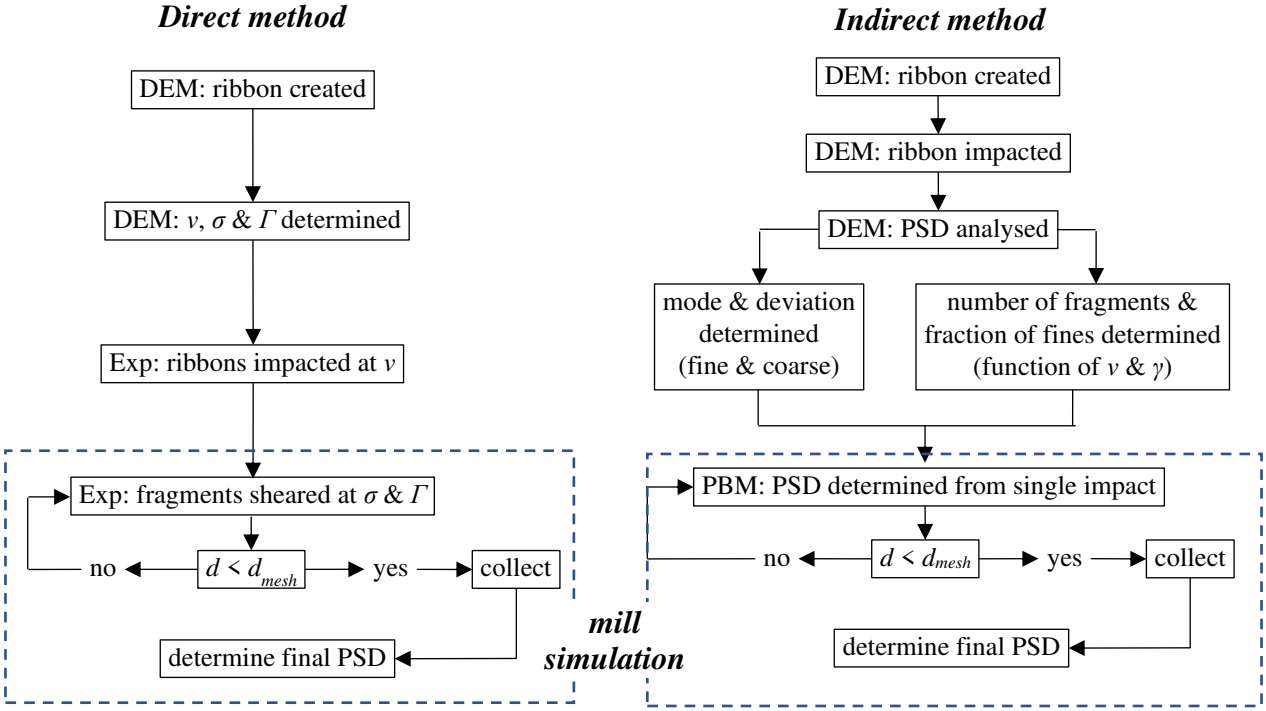

Figure 1. Steps in the two ribbon milling prediction approaches. v, γ, d, σ, Γ are impact velocity, surface energy, characteristic size, normal stress and shear strain, respectively.

2. The direct approach (Hare *et al.*, 2016)

2.1. Dominant breakage mechanism(s)

It was proposed that breakage in the mill is primarily due to the first impacts of the ribbons – either when colliding with the bar at the mill entrance or with the mesh at the base of the mill – and shearing of the ribbons/fragments against the mesh at the base of the mill. Secondary impacts were assumed negligible in the mill and so ignored in characterisation of the real ribbons.

2.2. Incorporation of particle bonds

Roller compacted ribbons were simulated using the DEM cemented-bond model of Brown *et al.* (2014), based on the Timoshenko (1922) beam theory. The ribbons were formed from a sheet of

monosize spheres of 0.9 or 0.45 mm radius (depending on the material represented), each separated by 1 μm, in a square packing arrangement of one particle diameter thickness. Adjacent spheres were bonded whilst diagonal neighbours were not, with all bond parameters being uniform throughout the entirety of all sheets.

2.3. Characterisation of bond strength

A three-point bend test was applied to characterise the strength of ten real ribbons, with the same test simulated using the same simulated ribbons defined in section 2.2. The bond strength was varied in separate simulations until the failure force was within 10% of the average experimental failure force.

2.4.Mill simulation

Eight ribbons as defined in section 2.2 were generated above the mill entrance. The mesh was represented as a solid hemi-cylindrical wall, attached to vertical side walls. The bars of the mill were rotated at a defined velocity, with the clearance between the bars and the mesh fixed at 1 mm. The force, F, acting on each bar was monitored throughout the simulation, with the normal stress applied to each ribbon assumed to equal this force divided by the projected area, A_p, of contact – taken as the square of the particle diameter multiplied by the number of spheres in contact with the bar, therefore:

$$\sigma = \frac{F}{\sum_{i}^{c} A_p} \qquad \text{(Eq. 1)}$$

where c is the total number of sphere contacts with the given bar. The shear strain, Γ, for each pass of the roller was determined using Equation 2.

$$\Gamma = \frac{V_r \cdot t}{d} \qquad \text{(Eq. 2)}$$

where V_r is the translational velocity of the bar, t is the duration of the shearing event (taken as the continuous period where $F > 0$) and d is the gap between the bar and the mill.

2.5.Prediction of breakage in the mill

To characterise the breakage behaviour due to shearing against the mesh, experiments were carried out using an annular shear cell to shear single layers of ribbon fragments that had experienced an impact event to represent their entry into the mill. The impact velocities that the ribbons were exposed to in the mill were determined by simulating impact of single sheets comprising clumped spheres with the particle arrangement described in section 2.2 (without the 1 μm spacing between neighbouring particles). Fifty ribbons were successively introduced into the mill to determine the average impact velocities of ribbons colliding with the bar at the mill entrance and those bypassing the bar and first impacting the base, as well as the percentage of ribbons attributed to these two scenarios. In the experiments, ten ribbons were individually impacted against a rigid surface by dropping from a height determined to provide the desired impact velocity. The impacted ribbons were sheared in the annular shear cell at the average normal stress and strain determined from the mill simulation. The material in the cell was then sieved using a mesh size representing the screen mesh of the real mill. All material passing through the sieve was collected for subsequent analysis whilst material remaining on the sieve was arranged in the annular shear cell and exposed to the same shearing conditions. This process was repeated until all material passed through the sieve. Sieve size analysis was then carried out for the collected material to predict the size distribution of the mill product.

2.6.Parameters varied

Two separate ribbon materials were experimentally characterised in the three-point bend, impact and shearing experiments. The mill speed and ribbon length were varied in the mill simulation in order to analyse their effects on the size distribution of the mill product.

3. The indirect approaches of Loreti *et al.* [14,15]

3.1. Dominant breakage mechanism(s)

Depending on the rotating speed of the pins in the mill, two dominant breakage mechanisms were identified: impact and abrasion [6]. Loreti *et al.* [14] analysed impact-dominant milling, while Loreti *et al.* [15] focused on abrasion-dominant breakage.

3.2. Incorporation of particle bonds

The auto-adhesive model of Thornton and Yin [18] was used to apply a surface energy to each particle, leading to adhesion between all contacting particles. A total of 1460 spheres, with diameters of 77 – 312 μm and an initial surface energy of zero, were generated within a parallelepiped geometry. The walls of the geometry were then moved inwards to confine the particle assembly and increase the packing fraction to a value of 0.74. A surface energy of 200 mJ/m^2 was then introduced to each particle. The surface energy was then gradually reduced to a prescribed value whilst the confinement of the walls was relaxed.

3.3. Characterisation of bond strength

Considering the approach by [14], the impact breakage behaviour of mannitol was experimentally determined by [19] and found to result in a bimodal size distribution. Breakage products smaller than 360 μm were classified as fines, whilst larger fragments were classed as fragments. The number of fragments, p, and the mass fraction of fines, z, were determined.

The DEM ribbon formed in section 3.2 was impacted against a surface by applying a fixed velocity to all particles. Following impact, the size distribution of the breakage products was determined by establishing which particles remained in contact after impact. Multiple simulations were carried out at various impact velocities and values of surface energy, with the values p and z determined for each simulation. The surface energy providing the closest fit to the experimental data for fines generated in the mill (z) across all investigated conditions was used in predicting the breakage behaviour in the mill.

[15] followed the same generation and breakage product analysis procedure, the difference being that the DEM model considered the ribbon agglomerate to be resting on a lower half box, with an upper half box resting against its surface translated at a given velocity, as shown in Figure 2.

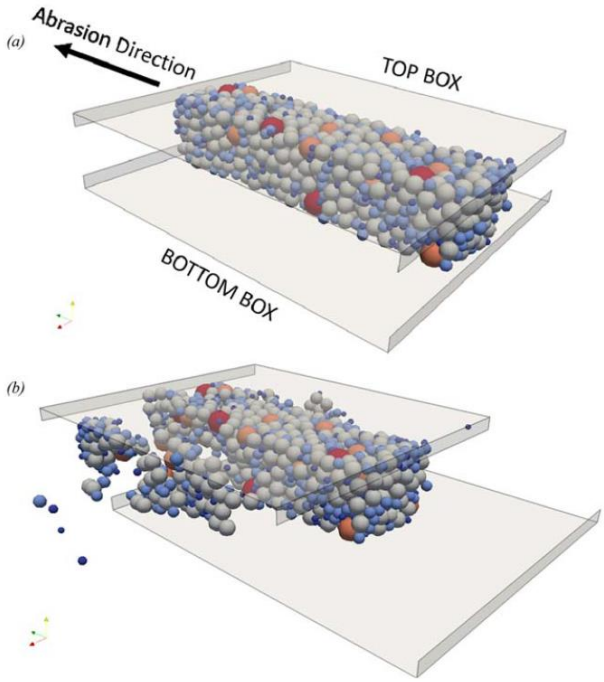

Figure 2. DEM abrasion model of Loreti *et al.* (2018)

3.4. Prediction of breakage in the mill

A population balance model (PBM) was used to predict the breakage behaviour in the mill. The impact velocity the ribbons were exposed to in the mill was assumed to be equal to that of the impeller tip speed and was therefore fixed in each case. The PBM determined the size distribution of breakage products after each impact event, with fragments that exceeded the mesh size being subjected to another impact. This process was iterated until no material greater than the screen size remained, following which the full size distribution was determined.

3.5. Parameters varied

The impeller tip speed and mill mesh size were varied in the PBM in both the impact and abrasion dominated breakage approaches.

4. Results & Discussion

Both approaches comprise a means of estimating both the strength of the real material and the extent of breakage of the material under mill operational conditions. In both approaches, the distributions of material strength and mill velocities, stresses or strains are not considered, with average values used for each. The method of strength characterisation is different in the two approaches, though both take an approach of varying bond/cohesion properties until a reasonable agreement with experimental data is found. [14] tested a range of surface energies and analysed the product size distribution after impact at a range of velocities with DEM, selecting the surface energy for the mill simulation that most closely agreed with the fines generated in experiments. [13] varied bond strength of the DEM ribbon to achieve a similar breakage force in a three-point bend test. For the mill simulation, both approaches consider all products from a single breakage event that exceed the mill mesh size to undergo a further breakage event; the process continuing until all material is below this mesh size, after which the product size distribution is determined. There is a distinct difference in the way that this is achieved in the two methods: [14] mathematically apply a population balance approach to analyse each breakage event, whilst [13] represent each breakage event experimentally in the shear cell.

In both approaches the prediction method is used to estimate aspects of the particle size distribution of the material exiting the mill and compare this to experimental data. [13] predict the size distribution of ribbons of 50 and 100 mm length at mill rotational speeds of 50 and 65 rpm, presented along with plant data for the mill with operational parameters within this range, as shown in Figure 3. The prediction agrees quite well with the plant data in the middle of the distribution (355 – 850 μm), with little influence of material and process parameters shown. The majority of the product is predicted to be > 1000 μm (50 – 65%), in reasonable agreement with plant data. The plant data shows less than 10% of product being fines (< 250 μm), whereas the simulation results predict 15-25% fines. As noted by [13], this fines overestimate could arise from several sources: (i) the fragments sheared in the shear cell were laid flat, whereas in the mill the fragments may not have settled on the screen following the previous shearing event prior to the next bar approaching; (ii) the grooves of the shear cell that ensure the fragments are gripped and sheared is not representative of the mill bar/screen interaction, and may lead to increased abrasion; (iii) in the shear cell the entire quantity of fragments and breakage products are sheared for the full strain of a shearing event, whereas in the mill any material smaller than the screen mesh size would have chance to exit the mill if percolated through and so would not experience further shearing.

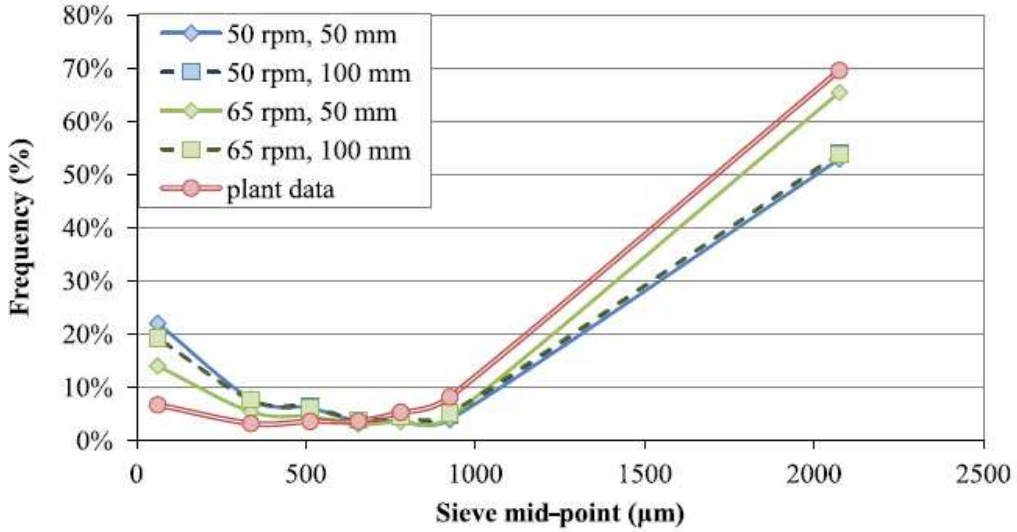

Figure 3. Mill product size distributions of Hare *et al.*, (2016)

Loreti *et al.* (2017) analysed the fraction of fines (< 360 μm) in the mill product at three impeller speeds (0.16, 0.33 and 0.65 m/s) and three mesh sizes (1.0, 1.5 and 2.0 mm) and compared to experimental data of [19], the results of which are shown in Figure 4. The DEM-PBM approach correctly predicted the influence of screen size, with a larger mesh resulting in a reduction in the fines fraction generated, and the difference being more significant for 1.0 to 1.5 mm than for 1.5 to 2.0 mm. Considering all impeller speeds, the prediction of fines fraction generated is approximately of the right magnitude; underestimated at low tip speeds and overestimated at high tip speeds. However, the prediction suggests a strong increase in the fine fraction with impeller speed, whereas no impeller speed effect is present in the experiments. As discussed by Loreti *et al.* (2017), this suggests that impact is not the dominant breakage mechanism, rather shear breakage dominates. Shear breakage is the breakage mechanism considered by Hare *et al.* (2016), whilst the further study by Loreti *et al.* (2018) considers abrasion dominated breakage, the results of which are shown in Figure 5. The range of values of the predicted fines fraction is closer to that of the experiments when considering abrasion dominant breakage behaviour; with the fines fraction agreeing well at low tip speeds for specific cases (2.0 mm mesh at 0.16 m/s and 1.5 mm mesh at 0.33 m/s), but

overestimating at higher tip speeds. However, the DEM-PBM approach still predicts a positive trend between fine fraction generated and impeller speed, meaning the influence of impeller speed is not correctly accounted for in the prediction. Whilst this discrepancy in the impeller speed effect is present for Loreti *et al.* (2017, 2018), such a comparison was not carried out by Hare *et al.* (2016), since only one experimental data set was considered, it therefore cannot be concluded whether this latter approach captures the effect of changing process parameters – an important capability of any predictive model. The experimental trend of Mirtič and Reynolds (2016), shown in Figure 4 and Figure 5, suggests that the dominant breakage mechanism and the conditions leading to breakage are almost independent of impeller speed. Shear-dominant breakage is a viable mechanism to fit this behaviour, since stress and strain may be independent of the tip speed, and breakage behaviour be independent of strain rate within the operational regime. The DEM predictions of stress and strain established by Hare *et al.* (2016), shown in

Table 1, do suggest a negligible influence of mill rotational speed on the average peak stress applied to the ribbons, however a reduction in shear strain with increasing mill speed is predicted, in contrast to the above hypothesis. The shear strain prediction relies on the assumptions that active shearing takes place for the full period where a non-zero stress is applied, and that the bar-screen clearance remains fixed at 1 mm. The duration of contact between the bar and the ribbon fragments in the DEM may be overestimated due to the representation of the ribbon by a single layer of primary particles, hence restricting the freedom of the fragments to exit the shear zone.

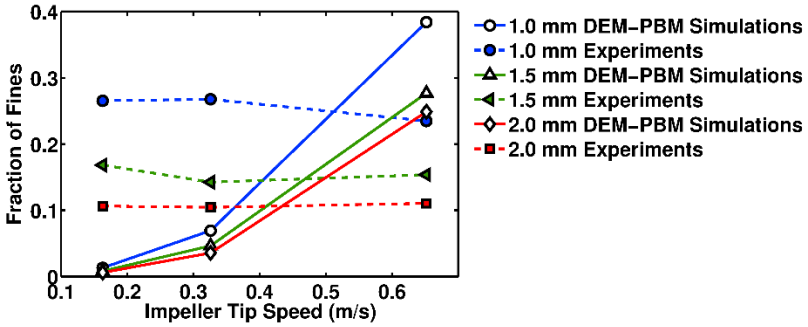

Figure 4. Mill product size distributions of Loreti *et al.*, (2017)

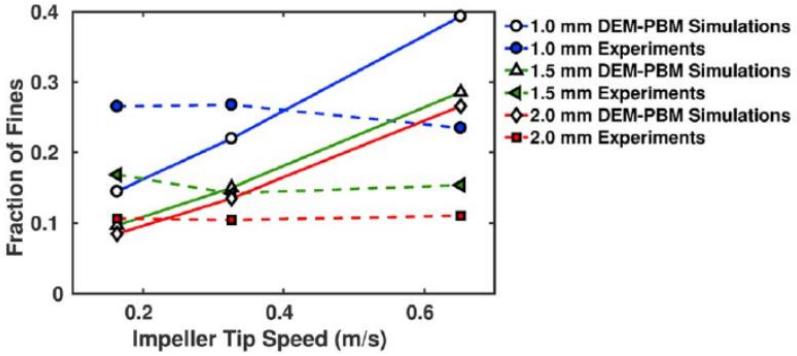

Figure 5. Mill product size distributions of Loreti *et al.* (2018)

Table 1. Characteristic normal stresses and shear strain in the DEM mill prediction of Hare *et al.* (2016)

Formula	A	A	A	A	B	B	B	B
Mill speed (rpm)	50	50	65	65	50	50	65	65
Sheet length (50 mm)	50	100	50	100	50	100	50	100
Max stress (kPa)	26.8	26.7	27.3	29.6	0.6	1.4	1.2	1.6
Average stress (kPa)	5.2	5.3	6.4	6.1	0.000	0.036	0.036	0.032
Average stress duration, t_{shear} (s)	0.19	0.22	0.08	0.1	0.05	0.03	0.03	0.02
Strain (−)	168	250	93	116	43	26	29	22
Angle of shear cell rotation (°)	124	184	68	85	–	–	–	–

One significant challenge in predicting breakage in such a milling process is accounting for the breakage from successive stressing events. Extensive research has been carried out by Kalman and co-workers (e.g. Rozenblat *et al.*, 2013; Uzi *et al.*, 2016) in characterising the change in breakage rates as particles and their fragments are successively impacted. When considering breakage of a ribbon, the fragments generated differ drastically in size and shape, and potentially strength, to the initial ribbon. As such, the distribution of breakage products following successive stressing events is likely to change as the process continues to break the ribbon down to fragments slightly larger than the screen mesh size. Furthermore, the precise arrangement of the fragments during a stressing event will vary as milling proceeds, particularly since the clearance between the mill bars/impellers and the screen is narrow, and the stochastic nature of this is difficult to capture in a PBM approach without extensive characterisation. In this respect the direct, experimentally determined breakage approach of Hare *et al.* (2016) is advantageous, however this also requires extensive experimental testing if the material does not completely break down to sizes smaller than the screen mesh within a few stressing events.

A major simplification in both approaches is the assumption of average values for stressing event parameters (impact velocities, stresses and strains) under a given mill operational condition. The stresses acting on the bars of the mill predicted by the DEM simulation of Hare *et al.* (2016), shown in Figure 6, show that the fluctuations of stress throughout the milling process are significant. Likewise, in an impact dominated breakage regime, due to the movement of fragments in the mill caused by previous impacts, the impact velocity and angle of inclination will inherently exhibit a distribution. By considering an average value for process parameters, this complexity is lost. To include the distribution requires a considerable experimental effort regardless of the prediction approach applied, though since the stochastic nature of breakage events is lost in the indirect approach, inclusion of the distribution of stressing event parameters may be of greater importance in such an approach.

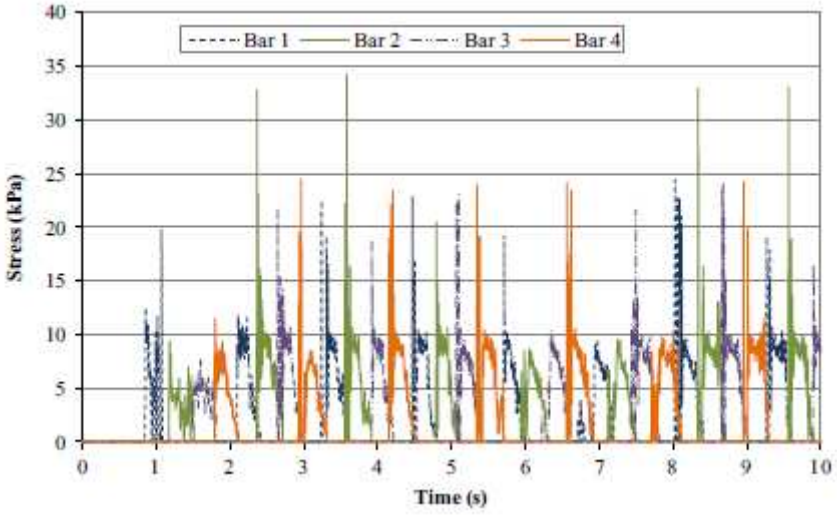

Figure 6. Normal stress profile throughout the mill simulation of Hare *et al.* (2016)

An alternative to the direct and indirect PBM approaches discussed so far is to directly incorporate the breakage into DEM [22]. An advantage this gives is that the stochastic interaction of particles and process, and therefore the distribution of stressing event parameters, are inherently incorporated in the breakage prediction. However, there are several challenges to such an approach: (i) accurate representation of the fragments, including size, shape and incident velocity following a breakage event, particularly in the chipping and abrasion breakage regimes; (ii) accurate characterisation of strength distribution, particularly taking into account the influence of loading direction and location of breakage points, and furthermore considering this for generated fragments; (iii) the number of fines generated can be too computationally expensive, this is compounded by the large size ratios present for a simulation containing fines and larger fragments (or unbroken feed material). The two former challenges can be overcome using an FDEM approach [11,12], however the computational expense increases dramatically, to such a degree that it is currently unviable for large mill simulations, particularly when considering the latter challenge of number of fines generated.

From the above discussion it is apparent that for an accurate breakage prediction model of a mill there is no avoiding the necessity of extensive experimental characterisation. Carrying out breakage characterisation that is relevant to the dominant breakage mechanism of the system is of critical importance. In such a system where more than one breakage mechanism has a significant contribution to overall breakage it is necessary to represent all such mechanisms in the experimental characterisation. A reasonable prediction of breakage products can be achieved when considering only average values for material strength and stressing event parameters, though accuracy is expected to improve by considering the distributions. The necessity of including the stressing parameter distribution is system dependent, and significantly increases the experimentation required to characterise breakage of the material under these conditions. Inclusion of the material strength distribution in the DEM requires a more sophisticated model to be developed, which mainly impacts the effort in setting up the simulation, with only a slight negative effect on the computational speed. One further effect not considered in either approach discussed in this paper is the variability of impeller/bar-screen clearance. Since the screen in this type of mill is flexible, the weight of the material in the mill causes a degree of flex that enhances the clearance size. Incorporation of such a flexible boundary in DEM has been achieved in other systems [23], though comes with some computational expense and a requirement to characterise the flexibility of the screen. A summary of these considerations, their perceived importance and difficulty to implement, and a comment on their presence in the discussed approaches are shown in Table 2.

Table 2. Summary of relevant features for ribbon milling prediction

Relevant features	Importance for prediction accuracy	Difficulty/expense to implement	Applied by Hare *at al.* [13]?	Applied byLoreti *et al.* [14,15]?
Shearing mechanism	high	low	yes	no
Ribbon average strength	high	low	yes	yes
Ribbon strength distribution	medium	medium	no – in DEM yes – in exp. mill model	no
Average stressing parameter	high	low-medium	yes	yes
Stressing parameter distribution	medium	medium-high	no	no
Ribbon thickness greater than primary particles	medium-high	medium-high	no	yes
Variable mesh-bar clearance	low-medium	high	no	no

5. Conclusions

Two DEM-PBM ribbon milling size distribution prediction approaches, one direct and the other indirect, have been outlined and contrasted. The indirect approach uses the PBM to determine the iterative shift in the size distribution after successive shearing events, whilst the direct approach uses experimentation to subject fragments to these successive shearing events. The direct approach results in a size distribution prediction that agrees reasonably well with plant data, though the influence of mill operational speed is not analysed experimentally. The indirect approach predicts the right magnitude of fines generated, though incorrectly predicts fines to increase with operational speed, rather than to be independent as shown by experiments. This discrepancy is attributed to the dominant breakage in the mill not having been captured in the indirect approach. The accuracy of the prediction is expected to improve for any method by including distributions of material strength and the stressing parameter. One advantage of the direct approach is that it directly accounts for the material strength distribution in the experimental component, as well as capturing the stochastic nature of fragment loading conditions and breakage behaviour during stressing events. Alternative approaches of directly incorporating breakage into DEM face challenges in accurately representing the fragments, incorporating the strength distribution whilst accounting for all relevant loading configurations and inclusion of the significant number of fines generated. Whether predicting breakage rates by an indirect or direct DEM-PBM method, or directly in the DEM, there is no avoiding the fact that an accurate prediction requires extensive experimental testing.

References

[1] M. Khorasani, J.M. Amigo, J. Sonnergaard, P. Olsen, P. Bertelsen, J. Rantanen, Visualization and prediction of porosity in roller compacted ribbons with near-infrared chemical imaging (NIR-CI), J. Pharm. Biomed. Anal. 109 (2015) 11–17. https://doi.org/https://doi.org/10.1016/j.jpba.2015.02.008.

[2] A.M. Miguélez-Morán, C.-Y. Wu, J.P.K. Seville, The effect of lubrication on density distributions of roller compacted ribbons, Int. J. Pharm. 362 (2008) 52–59. https://doi.org/https://doi.org/10.1016/j.ijpharm.2008.06.009.

[3] R.B. Al-Asady, J.D. Osborne, M.J. Hounslow, A.D. Salman, Roller compactor: The effect of mechanical properties of primary particles, Int. J. Pharm. 496 (2015) 124–136.

https://doi.org/https://doi.org/10.1016/j.ijpharm.2015.05.061.
[4] A. Vanarase, R. Aslam, S. Oka, F. Muzzio, Effects of mill design and process parameters in milling dry extrudates, Powder Technol. 278 (2015) 84–93. https://doi.org/https://doi.org/10.1016/j.powtec.2015.02.021.
[5] A.K. Samanta, K.Y. Ng, P.W.S. Heng, Cone milling of compacted flakes: Process parameter selection by adopting the minimal fines approach, Int. J. Pharm. 422 (2012) 17–23. https://doi.org/https://doi.org/10.1016/j.ijpharm.2011.10.015.
[6] S. Yu, M. Adams, B. Gururajan, G. Reynolds, R. Roberts, C.-Y. Wu, The effects of lubrication on roll compaction, ribbon milling and tabletting, Chem. Eng. Sci. 86 (2013) 9–18. https://doi.org/https://doi.org/10.1016/j.ces.2012.02.026.
[7] C. Thornton, L. Liu, How do agglomerates break?, Powder Technol. 143–144 (2004) 110–116. https://doi.org/10.1016/j.powtec.2004.04.035.
[8] D.O. Potyondy, P.A. Cundall, A bonded-particle model for rock, Int. J. Rock Mech. Min. Sci. 41 (2004) 1329–1364. https://doi.org/https://doi.org/10.1016/j.ijrmms.2004.09.011.
[9] P. Cleary, Modelling comminution devices using DEM, Int. J. Numer. Anal. Methods Geomech. 25 (2001) 83–105. https://doi.org/10.1002/1096-9853(200101)25:1<83::AID-NAG120>3.0.CO;2-K.
[10] T. Brosh, H. Kalman, A. Levy, Fragments spawning and interaction models for DEM breakage simulation, Granul. Matter. 13 (2011) 765–776. https://doi.org/10.1007/s10035-011-0286-z.
[11] G. Ma, W. Zhou, X.-L. Chang, Modeling the particle breakage of rockfill materials with the cohesive crack model, Comput. Geotech. 61 (2014) 132–143. https://doi.org/https://doi.org/10.1016/j.compgeo.2014.05.006.
[12] T. Luo, E.T. Ooi, A.H.C. Chan, S.J. Fu, The combined scaled boundary finite-discrete element method: Grain breakage modelling in cohesion-less granular media, Comput. Geotech. 88 (2017) 199–221. https://doi.org/https://doi.org/10.1016/j.compgeo.2017.03.012.
[13] C. Hare, M. Ghadiri, N. Guillard, T. Bosworth, G. Egan, Analysis of milling of dry compacted ribbons by distinct element method, Chem. Eng. Sci. 149 (2016) 204–214. https://doi.org/10.1016/j.ces.2016.04.041.
[14] S. Loreti, C.-Y. Wu, G. Reynolds, A. Mirtič, J. Seville, DEM–PBM modeling of impact dominated ribbon milling, AIChE J. 63 (2017) 3692–3705. https://doi.org/10.1002/aic.15721.
[15] S. Loreti, C.-Y. Wu, G. Reynolds, J. Seville, DEM–PBM modeling of abrasion dominated ribbon breakage, AIChE J. 64 (2018) 1191–1204. https://doi.org/10.1002/aic.16005.
[16] N.J. Brown, J.-F. Chen, J.Y. Ooi, A bond model for DEM simulation of cementitious materials and deformable structures, Granul. Matter. 16 (2014) 299–311. https://doi.org/10.1007/s10035-014-0494-4.
[17] P.S.P. Timoshenko, X. On the transverse vibrations of bars of uniform cross-section, London, Edinburgh, Dublin Philos. Mag. J. Sci. 43 (1922) 125–131. https://doi.org/10.1080/14786442208633855.
[18] C. Thornton, K.K. Yin, Impact of elastic spheres with and without adhesion, Powder Technol. 65 (1991) 153–166. https://doi.org/10.1016/0032-5910(91)80178-L.
[19] A. Mirtič, G.K. Reynolds, Determination of breakage rate and breakage mode of roller compacted pharmaceutical materials, Powder Technol. 298 (2016) 99–105. https://doi.org/https://doi.org/10.1016/j.powtec.2016.04.033.
[20] Y. Rozenblat, A. Levy, H. Kalman, I. Peyron, F. Ricard, A model for particle fatigue due to impact loads, Powder Technol. 239 (2013) 199–207. https://doi.org/https://doi.org/10.1016/j.powtec.2013.01.059.
[21] A. Uzi, H. Kalman, A. Levy, A novel particle attrition model for conveying systems, Powder Technol. 298 (2016) 30–41. https://doi.org/https://doi.org/10.1016/j.powtec.2016.05.014.
[22] N. Jiménez-Herrera, G.K.P. Barrios, L.M. Tavares, Comparison of breakage models in DEM in simulating impact on particle beds, Adv. Powder Technol. 29 (2018) 692–706. https://doi.org/https://doi.org/10.1016/j.apt.2017.12.006.

[23] G. Cheung, C. O'Sullivan, Effective simulation of flexible lateral boundaries in two- and three-dimensional DEM simulations, Particuology. 6 (2008) 483–500. https://doi.org/https://doi.org/10.1016/j.partic.2008.07.018.